

See discussions, stats, and author profiles for this publication at: <https://www.researchgate.net/publication/263292933>

# Structural Modeling of Ge<sub>6.25</sub>As<sub>32.5</sub>Se<sub>61.25</sub> Using a Combination of Reverse Monte Carlo and Ab Initio Molecular Dynamics

ARTICLE in THE JOURNAL OF PHYSICAL CHEMISTRY A · JUNE 2014

Impact Factor: 2.69 · DOI: 10.1021/jp5017856 · Source: PubMed

CITATIONS

2

READS

21

## 4 AUTHORS:



**George Opletal**

RMIT University

29 PUBLICATIONS 354 CITATIONS

SEE PROFILE



**Daniel W. Drumm**

RMIT University

17 PUBLICATIONS 69 CITATIONS

SEE PROFILE



**R.P. Wang**

Australian National University

168 PUBLICATIONS 1,479 CITATIONS

SEE PROFILE



**Salvy P Russo**

RMIT University

167 PUBLICATIONS 2,268 CITATIONS

SEE PROFILE

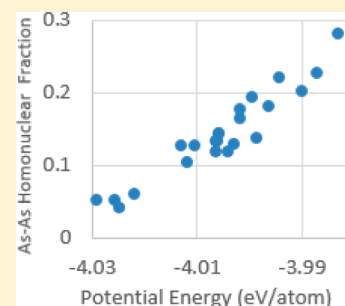
# Structural Modeling of $\text{Ge}_{6.25}\text{As}_{32.5}\text{Se}_{61.25}$ Using a Combination of Reverse Monte Carlo and Ab Initio Molecular Dynamics

George Opletal,<sup>\*,†</sup> Daniel W. Drumm,<sup>†</sup> Rong P. Wang,<sup>‡</sup> and Salvy P. Russo<sup>†</sup>

<sup>†</sup>Theoretical Chemical and Quantum Physics, School of Applied Sciences, RMIT University, 124 La Trobe Street, Melbourne, Victoria 3000, Australia

<sup>‡</sup>Centre for Ultrahigh Bandwidth Devices for Optical Systems (CUDOS), Laser Physics Centre, Research School of Physics and Engineering, The Australian National University, Canberra, Australian Capital Territory 0200, Australia

**ABSTRACT:** Ternary glass structures are notoriously difficult to model accurately, and yet prevalent in several modern endeavors. Here, a novel combination of Reverse Monte Carlo (RMC) modeling and ab initio molecular dynamics (MD) is presented, rendering these complicated structures computationally tractable. A case study ( $\text{Ge}_{6.25}\text{As}_{32.5}\text{Se}_{61.25}$  glass) illustrates the effects of ab initio MD quench rates and equilibration temperatures, and the combined approach's efficacy over standard RMC or random insertion methods. Submelting point MD quenches achieve the most stable, realistic models, agreeing with both experimental and fully ab initio results. The simple approach of RMC followed by ab initio geometry optimization provides similar quality to the RMC–MD combination, for far fewer resources.



## 1. INTRODUCTION

Germanium–arsenic–selenium (GeAsSe) chalcogenide glasses have received substantial interest over the past few decades due to their promising potential as photonic devices.<sup>1,2</sup> However, the performance of glass-based photonics devices always suffers from the structural relaxation intrinsic to disordered materials. Therefore, understanding the glass structure is essential to the fabrication of high-quality photonics devices. Unfortunately, experimental techniques only provide limited (but useful) clues to the bonding environments within these disordered systems, and thus computer simulations are invaluable in potentially providing a complete model of these glasses at the atomic level.

Numerous computational techniques have been applied to produce structural models of GeAsSe glasses; most notably the experimental-data-fitting Reverse Monte Carlo (RMC) methodology<sup>3</sup> for which numerous GeAsSe models exist<sup>4,5</sup> and models<sup>6–8</sup> produced by ab initio molecular dynamics (MD) methods such as density functional theory.<sup>9,10</sup> Both approaches present advantages and disadvantages.

The usefulness of the RMC technique is that it is computationally inexpensive and thus allows for large systems containing many thousands of atoms to be modeled. For nonporous glasses, this is generally sufficient to capture all the configurational environments characterizing the material. Additionally, experimental constraints (which minimize the discrepancy between experimentally obtained data and that calculated from the simulation) can be applied, producing atomic configurations consistent with such data. The primary disadvantage of the technique stems from the requirement of having sufficient experimental constraints to produce a unique configuration (labeled henceforth the uniqueness problem). For systems that can be completely modeled by a pairwise two-body interaction potential, a unique relationship exists between

the radial distribution function and the potential.<sup>11</sup> Under such conditions, it has been shown that the RMC methodology can reproduce Monte Carlo-simulation-generated structures from their radial distribution functions  $g(r)$ , identical in structural measures such as bond angle and ring-size distributions.<sup>12,13</sup> Unfortunately, for covalently bonded systems, this is not the case, and for many combinations of experimental constraints, there exist a multitude of atomic configurations that minimize them.

Structural models generated by density functional theory (DFT)-based molecular dynamics, while limited in size by computational expense, are inherently more accurate in their depictions of the local bonding than RMC simulations. To the best of our knowledge, there exist no empirical potentials for these ternary systems, and therefore modeling is limited to the more expensive first-principle methods. Typically, these MD models are produced by a melt and quench procedure where the system is cooled very rapidly (well above experimental cooling rates) from a high-temperature liquid state to a room-temperature glass. As is the case in GeAsSe glasses, problems arise when the liquid state has a radically different bonding environment to that of the cooled glass due to the rapid quench rate, “freezing in” artifacts from the liquid state. Cai et al.<sup>6</sup> have discussed the difficulty of modeling GeAsSe systems using this procedure while introducing their building block (BB) approach as a possible solution. In the BB approach, the main system cell is constructed via multiple replicas of smaller, repeatedly quenched, energetically relaxed building-block cells of only tens of atoms. The main cell is then heated up above

**Received:** February 19, 2014

**Revised:** May 31, 2014

**Published:** June 19, 2014



the melting point to remove any correlations between the building-block replicas with the assumption that the bonding was not overly changed at such a high temperature. A similar assumption was made in our previous work where the initial starting structures were instead RMC-generated models for the subsequent DFT MD simulations.<sup>7,8</sup>

One additional relevant methodology worthy of note is the Experimentally Constrained Molecular Relaxation (ECMR) method. This technique utilizes a structural optimization loop of repeated RMC followed by ab initio MD and has been used to develop accurate models of GeSe<sub>2</sub> systems.<sup>14,15</sup>

In this methodological study, we investigate

- The quality of models produced by the RMC methodology, RMC followed by DFT geometry optimization and RMC followed by expensive DFT MD simulations.
- The preservation of structural information from the RMC model following subsequent DFT geometry optimization and DFT MD as a function of temperature.
- The difficulty in using the quench-from-melt MD approach which has been reported to “freeze in” unphysical structure artifacts from the liquid state.<sup>6</sup>

## 2. METHODOLOGY

Two starting structures of Ge<sub>6.25</sub>As<sub>32.5</sub>Se<sub>61.25</sub> were generated using either the random-insertion (labeled RAN) or Reverse Monte Carlo (labeled RMC) method within the Hybrid Reverse Monte Carlo (HRMC) code.<sup>16,17</sup> Containing 240 atoms (15 Ge, 78 As, and 147 Se atoms) at an experimentally measured<sup>18</sup> density of 0.3549 atoms/Å<sup>3</sup>, this resulted in two periodic, simple-cubic cells with side lengths of 18.91 Å. According to the 8 − *N* rule, where *N* is the number of valence electrons, Ge, As, and Se are assumed to have 4, 3, and 2 neighbors, respectively. Under this assumption, which is supported by extended X-ray fine-structure studies (EXAFS) over a wide range of glass compositions,<sup>19,20</sup> the number of Se atoms within the system is theoretically just enough to saturate all of the Ge and As atomic bonds without any homonuclear bonding (Ge–Ge, As–As, Se–Se bonds). Such a glass is termed here a Se-even glass, as opposed to a Se-rich or Se-poor glass, and its concentration is given by 2*N*<sub>Ge</sub> + 1.5*N*<sub>As</sub> where *N*<sub>Ge</sub> and *N*<sub>As</sub> are the respective Ge and As concentrations.

The RAN model was generated by random insertion with the condition that no two atoms could be found within 2 Å of each other. The more-sophisticated RMC model used single-atomic-move Monte Carlo sampling to fit additional constraints imposed upon the system. These included

- Ge, As, and Se atoms being coordinated with 4, 3, and 2 nearest neighbors, respectively.
- The number of Ge–Ge or As–As bonds being minimized (supported by EXAFS studies—particularly in Se-even glasses<sup>20</sup>—illustrating that the majority of Ge and As bonds are with Se, while negligible amounts of Ge–Ge bonds and small amounts of Ge–As bonds are present).
- A fitting to the bond angle distribution *g*<sub>3</sub>(*θ*) and radial distribution function *g*(*r*) obtained from previous ab initio models<sup>7</sup> (since experimental data is largely absent and *g*<sub>3</sub>(*θ*) cannot be extracted by any known method). The justification for this approach is twofold. First, both the *g*(*r*) and *g*<sub>3</sub>(*θ*) are largely unchanged over a range of elemental compositions in the ab initio study and thus represent a good approximation to the expected *g*(*r*) in

the final models. Second, RMC models—despite fitting EXAFS and *g*(*r*) data—tend to produce broad, non-Gaussian *g*<sub>3</sub>(*θ*) distributions, even for models where there is minimal wide-angle Se–Se bonding.<sup>21</sup>

- The elimination of three-membered ring formation which can be an inherent artifact in RMC simulations.<sup>16</sup> Previously,<sup>7,8</sup> this was accomplished by excluding angles around 60° using the RMC++ code.<sup>22</sup> In this work, the HRMC code<sup>17</sup> without any empirical potential (RMC mode) was used, directly rejecting moves that locally produce a three-membered ring.

Both the RAN and RMC models were next used as initial starting structures in subsequent ab initio MD simulations using the Vienna ab initio simulation package (VASP).<sup>23</sup> For each starting structure, four initial temperatures and three quench rates were employed giving a total of 24 simulations and resulting models. With a glass transition temperature *T*<sub>g</sub> of 465 K and a melting point *T*<sub>m</sub> near 700 K for the chosen simulation stoichiometry, the initial temperatures sampled the temperature domains *T* > *T*<sub>m</sub> and *T*<sub>m</sub> > *T* > *T*<sub>g</sub>. Each simulation was first equilibrated at its initial temperature for a period of 19.2 ps (or 6400 ionic steps using a 3 fs time step). With the quench rates shown in Table 1, the long (L), medium (M) and

**Table 1. Starting Temperatures and Quench Rates (in K/ps) for the Subsequent Ab Initio MD Temperature-Quench Simulations for Both the RAN and RMC Initial Structural Models**

starting temperature (K)	short (S)	medium (M)	long (L)
2000	118.1	59.0	35.4
1500	83.3	41.7	25.0
1000	48.6	24.3	14.6
500	13.9	6.9	4.2

short (S) simulations were then quenched over 48, 28.8, and 14.4 ps, respectively, to 300 K followed by a 19.2 ps equilibration period at 300 K. As in previous studies,<sup>7,8</sup> the constant number of atoms, volume, and temperature (NVT) simulations were quenched using a Nosé–Hoover thermostat under the generalized-gradient approximation (GGA) using the Perdew–Wang (PW91) exchange-correlation functional,<sup>24</sup> ultrasoft pseudopotentials,<sup>25,26</sup> a plane-wave cutoff of 155.2 eV, and a 2 × 2 × 2 Monkhorst–Pack *k*-point sampling scheme,<sup>27</sup> with Methfessel–Paxton smearing<sup>28</sup> on the order of 2.

Following the MD simulations, determination of quantities such as elemental coordination, bonding-type fractions, nearest-neighbor bonding environment (BE) populations and distribution functions such as the radial distribution function were all calculated by averaging over 1500 frames or 4.5 ps at 300 K (apart from those of the initial RAN and RMC models, for which only a single configuration was used). A cutoff distance of 2.85 Å (found to be the minimum in the total and elemental partial *g*(*r*) curves between the first and second peaks) was used to define the nearest neighbors.

In order to calculate and compare the total energy of each resulting system and the initial RMC and RAN models, all the systems were internally geometry optimized using VASP at 0 K. Using the previously mentioned ab initio parameters, the conjugate-gradient minimization scheme was used, and energy minima were reached within 200 ionic steps (except for the initial RAN and RMC models, which took over 300). A single-point energy calculation using the tetrahedron smearing

Table 2. Averaged Analysis of Coordination and Bonding Types for the Initial RMC and RAN Models, As Well As after Geometry Optimization<sup>a</sup>

		coordination					bond type			
		1	2	3	4	5	Ge	As	Se	
$M_{\text{ELE}}$										
RMC										
Ge	4.00	0.0	0.0	0.0	100.0	0.0	0.0	3.3	96.7	
As	2.92	1.3	1.3	96.2	0.0	0.0	0.9	3.5	95.6	
Se	2.05	0.0	95.9	2.7	1.4	0.0	19.2	72.2	8.6	
$M_{\text{SYS}}$	2.46	0.4	59.2	32.9	7.1	0.0				
RMC (Optimized)										
Ge	3.80	0.0	0.0	20.0	80.0	0.0	0.0	3.5	96.5	
As	3.02	0.0	0.0	97.4	2.6	0.0	0.9	5.9	93.2	
Se	2.03	2.7	91.2	6.1	0.0	0.0	18.4	73.6	8.0	
$M_{\text{SYS}}$	2.47	1.7	55.8	36.7	5.8	0.0				
RAN										
Ge	2.80	0.0	33.3	33.3	20.0	6.7	9.5	38.1	52.4	
As	2.58	18.0	23.1	26.9	21.8	5.1	7.5	26.3	66.2	
Se	2.75	12.3	24.7	31.5	17.8	9.6	5.2	33.0	61.8	
$M_{\text{SYS}}$	2.70	13.4	24.7	30.1	19.2	8.0				
RAN (Optimized)										
Ge	3.67	0.0	6.7	20.0	73.3	0.0	10.9	34.5	54.5	
As	3.01	1.3	0.0	94.9	3.8	0.0	8.1	31.5	60.4	
Se	2.05	2.7	89.8	6.8	0.7	0.0	9.9	47.0	43.1	
$M_{\text{SYS}}$	2.47	2.1	55.4	36.2	6.2	0.0				
2000 K (RMC)										
Ge	2.69	10.1	31.6	37.0	17.8	2.7	1.4	18.6	80.0	
As	2.84	4.2	30.0	45.4	17.6	2.6	3.4	26.8	69.8	
Se	2.11	17.4	49.8	26.6	4.9	0.4	10.1	48.2	41.7	
$M_{\text{SYS}}$	2.43	12.9	42.2	33.4	9.8	1.2				
2000 K (RAN)										
Ge	2.73	8.0	32.8	37.2	18.6	2.7	1.9	16.9	81.3	
As	2.81	4.8	31.1	44.1	16.9	2.7	3.2	28.5	68.3	
Se	2.17	18.7	50.0	26.0	4.5	0.4	10.5	47.2	42.3	
$M_{\text{SYS}}$	2.41	13.5	42.8	32.6	9.4	1.3				

<sup>a</sup>Also shown are the statistics of the RMC and RAN models after MD equilibration at 2000K.  $M_{\text{SYS}}$  represents the percentage of atoms having a specific coordination irrespective of element type. The  $M_{\text{ELE}}$  column gives the average coordination for individual elements within a system. The 2000 K values are an average over 1500 configurations (4.5 ps), while the rest are obtained from single configurations. Values other than the average coordination numbers in the first column are percentages.

method with Blöchl's corrections<sup>29</sup> and plane-wave cutoff of 550 eV gave the total energies. Determination of the duly optimized RAN and RMC structures' properties was then undertaken via single configurations as for their initial models.

### 3. RESULTS AND DISCUSSION

The presentation of results is divided into three subsections. The first discusses the initial starting structures, and the effects of geometry optimization on them along with properties of the high-temperature liquid state. The second section focuses on the bonding environments present in the quenched MD models and the preservation of the initial structure from which they started as a function of quench rate and starting temperature. The final section discusses the potential energy calculated for all the MD systems after geometry optimization and presents some observed bonding trends and details of the lowest energy models.

**A. Initial Structures and Geometry Optimization.** In investigating the influence of the initial structures upon the resulting models, an ideal starting point is to present the coordination and bonding distributions of the initial RMC and RAN models along with that of their liquid states. These liquid states were calculated after the initial 19.2 ps equilibration at

2000 K as detailed earlier (prequench). Table 2 also shows these distributions for the starting structures after geometry optimization.

Lowering the systems' energy results in locally more-realistic bond angles and atomic distances without significant atomic rearrangement. This approach dramatically improves the RAN model's  $g(r)$  (see Figure 1) and elemental-coordination distributions (see Table 2). At the same time, because of the lack of significant atomic rearrangement, the bonding-type distributions are largely unchanged and unrealistic.

On the other hand, the original RMC model, which already had an accurate fit to the  $g(r)$  and was constrained to have more-realistic coordination and bond-type distributions from the beginning, is only minimally altered.

It is worth reflecting on the accuracy of this optimized RMC model. It fits the correct density, elemental concentration, coordination distribution, and has few homonuclear bonds, being dominated by  $\text{GeSe}_4$  tetrahedra and  $\text{AsSe}_3$  pyramidal structural units. It fits the  $g(r)$  and the bond angle distribution and, unlike all published RMC models of these glasses, it is energetically relaxed. Its total energy is found to be  $-4.00$  eV/atom (optimized RAN  $-3.92$  eV/atom) in good agreement with the later-discussed MD models, which all fall around  $-4.0$



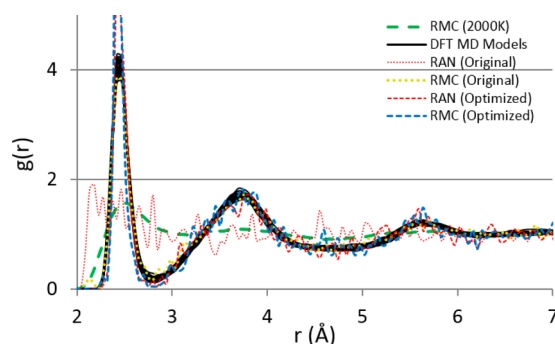


**Figure 1.** Individual  $g(r)$  for all DFT MD systems (note the similar behavior). The  $g(r)$  for the initial and geometry-optimized models of both the RAN and RMC models are also shown along with the  $g(r)$  in the liquid state (2000 K). The noisy curves for the original and optimized RAN and RMC models are due to the  $g(r)$  being calculated from a single configuration. The other curves are averaged over 1500 configurations.

eV/atom. Without geometry optimization, these values are higher (−3.77 and −3.12 eV/atom for RMC and RAN, respectively), illustrating the difficulty involved with modeling purely via the RMC methodology and ensuring that simulations are sufficiently constrained to produce realistic models of these glasses.

### B. Preservation of Initial Structure during Quench.

Prior to the discussion of the resulting models at the various starting temperatures and quench rates, it is informative to look at the effect the initial MD equilibration phase has on the RAN and RMC models at high temperatures before initiation of the quench. It is observed (see Table 2) that the liquid states at 2000 K (similarly for 1500 K and 1000 K, though not shown) are very similar for both the starting RAN and RMC models in terms of the bond-type and coordination distributions and their BE populations (and markedly different to the initial structures), indicating that at temperatures above  $T_m$  the initial structures are transformed to that of the liquid state. This liquid state thus becomes the new starting structure for the subsequent MD quench. However, since the bonding environment in the liquid is radically different from that of room-temperature systems, we run into the issue of “freezing in” unrealistic bonding environments from the liquid state and the previously mentioned difficulty of making accurate models using the melt and quench approach.<sup>6</sup>

Figures 2 and 3 show the dominant nearest-neighbor bonding environments found in the various models after the quench to, and equilibration at, 300 K. The BE populations of the initial and relaxed structures are also shown along with the BE populations of the liquid states at 2000 K. The first obvious observation (in line with the coordination and bonding distributions of Table 2) is how significantly different the 2000 K melt (red lines in the figures) is from the starting RMC model or the resulting MD models. This was further highlighted in Figure 1 where the  $g(r)$  values for the 24 systems were largely uniform and similar to previously published results<sup>6,7</sup> and experimental data,<sup>4</sup> yet very different from the 2000 K liquid state.

As a result, quenching from this high temperature can preserve some remnant bonding for the shortest simulations, as can be seen in the Se–As<sub>2</sub> population for both the RAN and RMC starting structures. In the case of the RMC model, the 2000 K liquid state has a vastly lower BE population of Se–As<sub>2</sub>

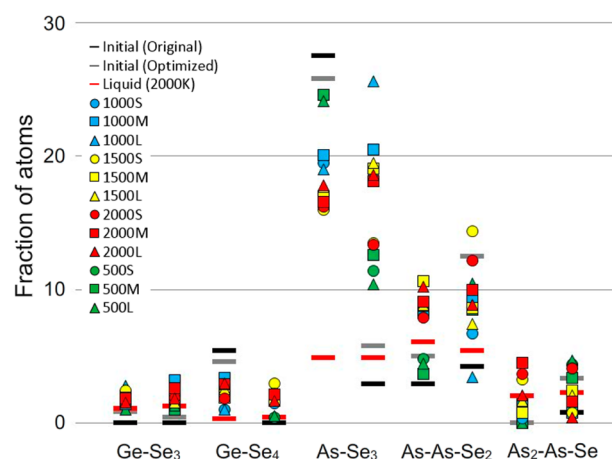


**Figure 2.** Dominant nearest-neighbor bonding environments for Ge and As atoms. For each BE type, the left data represents models derived from the RMC initial model, while the right represents the models derived from the RAN initial model. The black represents the initial RMC and RAN models, while the gray represents these two models after geometry optimization. The red line represents the values found in the 2000 K liquid prior to quenching in MD.

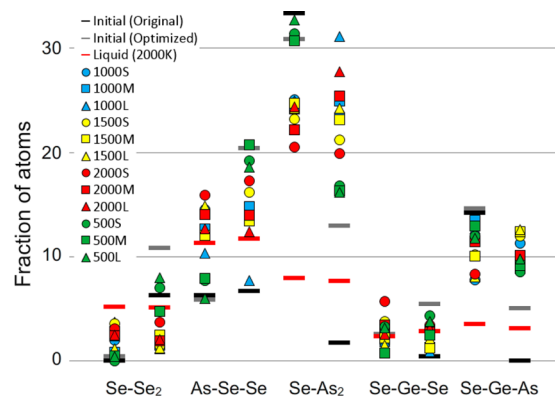


**Figure 3.** Dominant nearest-neighbor bonding environments for Se atoms. For each BE type, the left data represents models derived from the RMC initial model, while the right represents models derived from the RAN initial model. The black represents the initial RMC and RAN models, while the gray represents these two models after geometry optimization.

(7.9%) than that of the starting RMC model (33.3%) or the resulting MD models. As such, the shortest simulations (2000S) with the fastest quench rates tend to be closest to the starting liquid, followed by the medium (2000M) and long simulations (2000L). There is also a clear separation of MD models that were quenched from above the melting point (1000 K, 1500 K, and 2000 K simulations) and the 500 K simulations below the melting point. In the case of the RAN model, the initial structure is unphysical with a Se–As<sub>2</sub> population at 1.7%, and the subsequent MD quenches increase this value with increasing simulation length.

On the other hand, quenching from 500 K, which is just above  $T_g$  (and well below  $T_m$ ), results in models highly dependent on the initial structure. Looking again at the Se–As<sub>2</sub> BE populations, one can see that the 500S, 500M, and 500L values are closest to the original RMC value of 33%. A similar situation occurs for the RAN models that are trapped closest to the unphysical starting structure. Similar trends are found in the other BE environments including the most numerous BE, that

of As–Se<sub>3</sub>. Again, a similar grouping of simulations above the melting point is observed, which are separated from the 500 K simulations.

We therefore deduce that the use of a quench temperature above the melting point of the glass is proscribed in this case—and should potentially be so in others also, in agreement with Cai et al.<sup>6</sup> In any case, due care should be given to establishing whether artifacts in the model result from the phase change during the process, or are fortuitously preserved due to the choice of a short time scale, or genuinely represent the material being studied.

**C. Structural Features and Energies of Resulting Models.** After geometry optimization of all the MD models that were equilibrated at 300 K, potential energies were calculated and are shown in Figures 4 and 5 alongside the

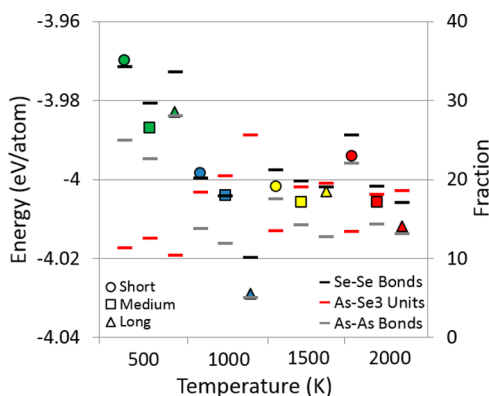


**Figure 4.** Energies for the RAN models along with the values within each model of the percentage of Se–Se and As–As bonds (from Se and As atoms, respectively) and the percentage of atoms having the As–Se<sub>3</sub> structural unit.

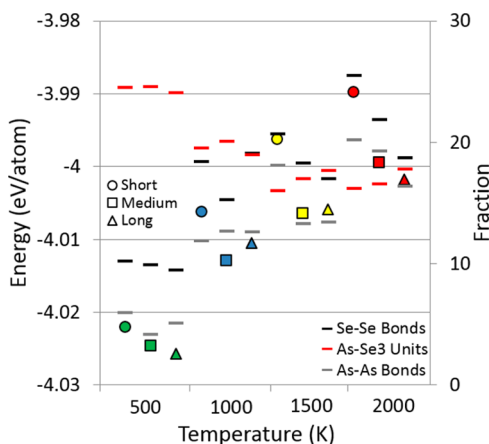


**Figure 5.** Energies for the RMC models along with the values within each model of the percentage of Se–Se and As–As bonds (from Se and As atoms, respectively) and the percentage of atoms having the As–Se<sub>3</sub> structural unit.

percentage of Se–Se bonds and As–Se<sub>3</sub> BE units. All of the models are within 0.06 eV/atom of each other and the geometry-optimized RMC model (–4.00 eV/atom). They are lower than the unoptimized RMC (–3.77 eV/atom) and RAN (–3.12 eV/atom) starting structures and the geometry optimized RAN model (–3.92 eV/atom).

Among the resulting MD models, a number of trends are observed. The first is that lower-energy structures correlate with

lower levels of Se–Se bonds. In addition, lower energies also correlate with high levels of As–Se<sub>3</sub> populations. Taken together, these findings support the idea that in Se-even glasses, there is minimal homonuclear bonding, and the system is largely composed of As–Se<sub>3</sub> (and Ge–Se<sub>4</sub>) structural units with a minimal population of Se dimers. Some Se–Se bonding is always present, as was found in previous simulations which showed a linear relationship between Se concentration and the number of Se–Se bonds even in Se-poor glasses.<sup>7</sup> As–As homonuclear bonding is also at minimal levels (around 5% as shown in Table 3) within the lowest-energy structures which is counter to the recent RMC model<sup>5</sup> of Ge<sub>5</sub>As<sub>30</sub>Se<sub>65</sub>, which fit X-ray diffraction and EXAFS data but contained a significant percentage of As–As bonding (46%). The authors there illustrated improved RMC fits to EXAFS data when As–As bonding was allowed, and their resulting model also contained a high fraction of Se–Se bonds (47%). Such high fractions of homonuclear bonding were not found in any of the resulting MD models.

The lowest-energy models were produced from a RMC initial structure followed by a quench from 500 K with the longer simulations obtaining a lower energy. This approach, which avoids the structural difficulties of quenching from the liquid state, suggests that RMC followed by DFT MD above the glass transition temperature but below the melting point is a viable way of preserving some of the initial RMC starting properties. Quenching from 500 K starting from the RAN structure results in the highest-energy structures, illustrating that some parts of the unphysical starting structure are preserved. One notable outlier is the 1000L RAN system. This obtained a low-energy, high As–Se<sub>3</sub> population, and low Se–Se bond population, and is structurally comparable with the RMC-initialized 500 K systems. A summary of the bonding environments within these lowest energy systems is shown in Table 3. Of these four systems, the RMC 500L system (which exhibits the highest Ge coordination of 3.79) is most closely consistent with EXAFS data requiring a 4-fold coordination for Ge atoms.<sup>19,20</sup>

#### 4. CONCLUSION

Ge<sub>6.25</sub>As<sub>32.5</sub>Se<sub>61.25</sub> glasses were produced by a combination of RMC and DFT MD simulations, and the structure and energetics were characterized against a variety of temperature quenching techniques. The primary findings were as follows:

- Models created from RMC alone, even with information that is not obtainable from experimental techniques such as the bond-angle distribution or elemental bonding fractions, have a significantly higher energy than all DFT MD models. This highlights the difficulty in employing the RMC methodology without any energetic constraints.
- In contrast, RMC models after DFT geometric optimization agree very well with DFT MD for total energy while largely retaining their RMC fits to the bond type and coordination distributions and represent a relatively computationally inexpensive (compared to DFT MD) technique to improve RMC models.
- Models created by a DFT MD quench from the liquid state, which is significantly structurally different to the room-temperature glass, tend to trap in unphysical structural bonding environments when using the highest quench rates.

Table 3. Averaged Analysis of Coordination and Bonding Types for the Four Lowest-Energy Models<sup>a</sup>

		Coordination					Bond Type		
	mean	1	2	3	4	5	Ge	As	Se
RMC 500L									
Ge	3.79	0.1	2.2	16.8	80.9	0.0	0.0	7.0	93.0
As	3.07	0.0	0.3	92.8	6.8	0.1	1.7	5.1	93.2
Se	2.07	0.6	91.7	7.5	0.2	0.0	17.3	73.2	9.5
mean	2.50	0.4	56.4	35.8	7.4	0.0			
RMC 500M									
Ge	3.62	0.1	6.0	25.7	68.2	0.0	0.0	7.4	92.6
As	3.07	0.0	0.5	92.2	6.9	0.3	1.7	4.2	94.2
Se	2.08	1.4	89.3	9.0	0.3	0.0	16.4	73.7	9.9
mean	2.50	0.8	55.3	37.1	6.7	0.1			
RMC 500S									
Ge	3.69	0.4	3.5	33.1	73.3	0.0	0.0	7.1	93.0
As	3.05	0.0	0.4	94.2	5.3	0.1	1.6	6.0	92.4
Se	2.06	1.1	92.2	6.6	0.1	0.0	17.0	72.8	10.8
mean	2.48	0.7	56.8	36.1	6.4	0.0			
RAN 1000L									
Ge	3.50	0.3	6.2	37.2	56.1	0.2	0.0	3.8	96.2
As	3.07	0.0	0.2	93.3	6.4	0.2	0.8	5.1	94.1
Se	2.08	1.0	89.8	9.1	0.1	0.0	16.5	73.4	10.1
mean	2.49	0.6	55.4	38.2	5.6	0.1			

<sup>a</sup> $M_{\text{SYS}}$  represents the percentage of atoms having a specific coordination irrespective of element type.  $M_{\text{ELE}}$  represents the average coordination for individual elements within a system. All values are an average over 1500 configurations (4.5 ps) at 300 K. Values other than the average coordination numbers in the first column are percentages.

- (iv) The lowest-energy configurations resulted from a combination of RMC initial structures and an MD quench from a temperature above the glass transition temperature but below that of melting. This may represent a viable modeling approach to preserve the RMC fit experimental information while relaxing the structure energetically using accurate DFT calculations.
- (v) Of all the models, the lowest energy systems contained the least amount of Se–Se and As–As homonuclear bonding and the highest fraction of As–Se<sub>3</sub> nearest-neighbor environments, which is consistent with past EXAFS studies.<sup>20</sup>

## AUTHOR INFORMATION

### Corresponding Author

\*E-mail: george.opletal@rmit.edu.au.

### Present Address

Theoretical Chemical and Quantum Physics, School of Applied Sciences, RMIT University. 124 La Trobe Street, Melbourne, Victoria 3000, Australia.

### Notes

The authors declare no competing financial interest.

## ACKNOWLEDGMENTS

We are grateful for funding support from the Australian Research Council (ARC) Centre of Excellence to the Centre for Ultrahigh Bandwidth Devices for Optical Systems (CUDOS) and the ARC discovery project DP110102753. In addition, we are thankful to the National Computational Infrastructure (NCI) for the computational resources required for this study.

## REFERENCES

- (1) Hisakuni, H.; Tanaka, K. Optical Microfabrication of Chalcogenide Glasses. *Science* **1995**, *270*, 974–975.
- (2) Saitoh, A.; Tanaka, K. Self-Developing Aspherical Chalcogenide-Glass Microlenses For Semiconductor Lasers. *Appl. Phys. Lett.* **2003**, *83*, 1725–1727.
- (3) Pusztai, L.; McGreevy, R. L. MCGR: An Inverse Method for Deriving the Pair Correlation Function from the Structure Factor. *Phys. B* **1997**, *234*, 357–358.
- (4) de la RosaFox, N.; Esquivias, L.; Villares, P.; Jimenez-Garay, R. Structural Models of the Amorphous Alloy Ge<sub>0.20</sub>As<sub>0.40</sub>Se<sub>0.40</sub> by a Random Technique. *Phys. Rev. B* **1986**, *33*, 4094–4099.
- (5) Kaban, I.; Jovari, P.; Wang, R. P.; Luther-Davies, B.; Mattern, N.; Eckert, J. Structural Investigations of Ge<sub>3</sub>As<sub>x</sub>Se<sub>95-x</sub> and Ge<sub>15</sub>As<sub>x</sub>Se<sub>85-x</sub> Glasses Using X-ray Diffraction and Extended X-ray Fine Structure Spectroscopy. *J. Phys.: Condens. Matter* **2012**, *24*, 385802/1–385802/10.
- (6) Cai, B.; Zhang, X.; Drabold, D. A. Building Block Modelling Technique: Application to Ternary Chalcogenide Glasses g-Ge<sub>2</sub>As<sub>4</sub>Se<sub>4</sub> and g-AsGe<sub>0.8</sub>Se<sub>0.8</sub>. *Phys. Rev. B* **2011**, *83*, 092202/1–092202/4.
- (7) Opletal, G.; Wang, R. P.; Russo, S. P. Bonding Trends Within Ternary Isocoordinate Chalcogenide Glasses Ge<sub>x</sub>As<sub>y</sub>Se<sub>(1-x-y)</sub>. *Phys. Chem. Chem. Phys.* **2013**, *15*, 4582–4588.
- (8) Opletal, G.; Wang, R. P.; Russo, S. P. Investigation of Bonding Within Ab-Initio Models of GeAsSe Glasses. *Chem. Phys. Lett.* **2013**, *575*, 97–100.
- (9) Hohenberg, P.; Kohn, W. Inhomogeneous Electron Gas. *Phys. Rev.* **1964**, *136*, B864–B871.
- (10) Kohn, W.; Sham, L. J. Self-Consistent Equations Including Exchange and Correlation Effects. *Phys. Rev.* **1965**, *140*, A1133–A1138.
- (11) Henderson, R. L. A Uniqueness Theorem for Fluid Pair Correlation Functions. *Phys. Lett. A* **1974**, *49*, 197–198.
- (12) Pusztai, L.; Tóth, G. On the Uniqueness of the Reverse Monte Carlo Simulation. I. Simple Liquids, Partial Radial Distribution Functions. *J. Chem. Phys.* **1991**, *94*, 3042–3049.

- (13) Shick, A.; Rajagopalan, R. Reverse Monte Carlo Procedure for Cluster Analysis in Colloidal Systems. *Colloids Surf.* **1992**, *66*, 113–119.
- (14) Biswas, P.; Tafen, D.; Drabold, D. A. Experimentally Constrained Molecular Relaxation: The Case of Glassy GeSe<sub>2</sub>. *Phys. Rev. B* **2005**, *71*, 054204/1–054204/5.
- (15) Drabold, D. A. Topics in the Theory of Amorphous Materials. *Eur. Phys. J. B* **2009**, *68*, 1–21.
- (16) Opletal, G.; Petersen, T. C.; O'Malley, B.; Snook, I.; McCulloch, D. G.; Marks, N.; Yarovsky, I. Hybrid Approach for Generating Realistic Amorphous Carbon Structures Using Metropolis and Reverse Monte Carlo. *Mol. Simul.* **2002**, *28*, 927–938.
- (17) Opletal, G.; Petersen, T. C.; Snook, I. K.; Russo, S. P. HRMC\_2.0: Hybrid Reverse Monte Carlo Method With Silicon, Carbon and Germanium Potentials. *Comput. Phys. Commun.* **2013**, *184*, 1946–1957.
- (18) Wang, R. P.; Luther-Davies, B. *Amorphous Chalcogenides: Advances and Applications*; Pan Stanford Publishing: Singapore, 2014; Chapter 4, pp 97–141.
- (19) Sen, S.; Aitken, B. G. Atomic Structure and Chemical Order in Ge–As Selenide and Sulfoselenide Glasses: An X-ray Absorption Fine Structure Spectroscopic Study. *Phys. Rev. B* **2002**, *66*, 134204/1–134204/10.
- (20) Wang, T.; Wang, R. P.; Luther-Davies, B. EXAFS Study of the Local Order in Ge–As–Se Glasses. *Phys. Proc.* **2013**, *48*, 89–95.
- (21) Opletal, G.; Russo, S. P. *Amorphous Chalcogenides: Advances and Applications*; Pan Stanford Publishing: Singapore, 2014; Chapter 5, pp 143–167.
- (22) Gereben, O.; Jóvári, P.; Temleitner, L.; Pusztai, L. A New Version of the RMC++ Reverse Monte Carlo Programme, Aimed at Investigating the Structure of Covalent Glasses. *J. Optoelectron. Adv. Mater.* **2007**, *9*, 3021–3027.
- (23) Kresse, G.; Furthmüller, J. Efficiency of Ab-Initio Total Energy Calculations for Metals and Semiconductors Using a Plane-Wave Basis Set. *Comput. Mater. Sci.* **1996**, *6*, 15–50.
- (24) Perdew, J. P.; Wang, Y. Accurate and Simple Analytic Representation of the Electron–Gas Correlation Energy. *Phys. Rev. B* **1992**, *45*, 13244–13249.
- (25) Vanderbilt, D. Soft Self-Consistent Pseudopotentials in a Generalized Eigenvalue Formalism. *Phys. Rev. B* **1990**, *41*, 7892–7895.
- (26) Kresse, G.; Hafner, J. Norm-Conserving and Ultrasoft Pseudopotentials for First-Row and Transition Elements. *J. Phys.: Condens. Matter* **1994**, *6*, 8245–8257.
- (27) Monkhorst, H. J.; Pack, J. D. Special Points for Brillouin-Zone Integrations. *Phys. Rev. B* **1976**, *13*, 5188–5192.
- (28) Methfessel, M.; Paxton, A. T. High-Precision Sampling for Brillouin-Zone Integration in Metals. *Phys. Rev. B* **1989**, *40*, 3616–3621.
- (29) Blöchl, P. E.; Jepsen, O.; Andersen, O. K. Improved Tetrahedron Method for Brillouin-Zone Integrations. *Phys. Rev. B* **1989**, *49*, 16223–16233.